



The Calibration and Evaluation of 50 cm Box and Line Photomultiplier Tubes Designed for Hyper-Kamiokande

Junjie XIA¹, Yasuhiro NISHIMURA¹, Christophe BRONNER², Toshiki MOCHIZUKI¹
for Hyper-Kamiokande Proto-Collaboration

¹*Institute for Cosmic Ray Research (ICRR), The University of Tokyo, 5-1-5 Kashiwanoha, Kashiwa, Chiba, 277-8582, Japan*

²*Kamioka Observatory, Higashi-Mozumi 456, Kamioka-cho, Hida-city Gifu 506-1205, Japan*

E-mail: seanxia@icrr.u-tokyo.ac.jp

(Received March 25, 2019)

Before the 2018 Super-Kamiokande (SK) detector upgrade, a hundred and forty-five 50 cm Box and Line (B&L) photomultiplier tubes (PMTs) have been carefully checked and measured in a laboratory near to the SK tank. Through various investigations including charge and timing response, required voltage, dark rate, etc., we have concluded that all received B&L PMTs were of good quality to be installed inside SK. In total 136 B&L PMTs have been picked at random and installed to replace the old SK PMTs.

KEYWORDS: Photomultiplier Tube, Water Cherenkov Detector

1. Introduction

Hyper-Kamiokande (HK), the next generation of underground water Cherenkov detector, is eight times larger in fiducial volume than its predecessor—SK. In HK, there will be around 40,000 new 50 cm B&L PMTs (Hamamatsu R12860) looking at the inner tank. The term “Box and Line” stands for the PMT’s dynode plate arrangement, which is known for good photon coverage and linearity in charge response. At $\lambda = 390$ nm, thanks to its better photocathode the HK B&L PMT was measured to have a quantum efficiency (QE) at around 30% compared to that of SK Venetian blind PMT’s (Hamamatsu R3600) at 22%. Additionally the photon collection efficiency (CE), which was an issue for the blind dynode structure, has also increased from $\sim 73\%$ to $\sim 95\%$. Therefore these improvements make a great contribution to the 1.9 times better photon detection efficiency of the HK B&L PMT. Meanwhile there are several fundamental requirements for the new PMTs, i.e. charge resolution $\leq 50\%$, timing resolution (FWHM) ≤ 5.2 ns¹, PMT gain $\geq 10^7$, etc [1]. To verify the quality of a recent production, we investigated a sample group of the HK B&L PMTs.

2. Experimental Method

2.1 Experimental Setup

A dark room surrounded by Helmholtz coils in all three spatial directions was set up to measure seven PMTs simultaneously. We kept one PMT as the reference at channel 7 throughout the whole experiment while replacing the six others everyday. The entrance of the dark room was defined as the -Y direction and the normal of ground as the +Z direction. Fig.1 demonstrates the layout inside the dark room with all seven PMT channels and positions. PMTs were kept pointing to the +Z direction. All PMT dynodes were aligned in the same direction to control the systematic uncertainties that may

Here the resolutions refer to the value measured at Single Photoelectron (SPE).



originate from the photoelectron trajectory, which is sensitive to magnetic field.

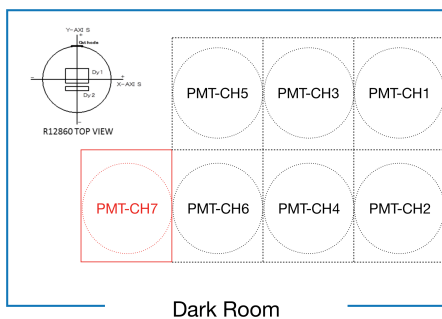


Fig. 1. The setup of channels and coordinates inside the dark room. PMT-CH7 was fixed with the same tube.

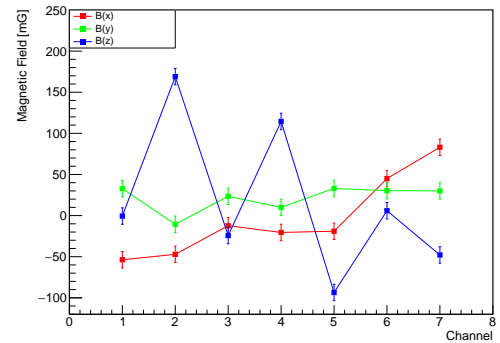


Fig. 2. The magnetic field at each channel inside the dark room.

Directly above all the PMTs, optical fibers connected to a single laser-diode (LD) were hanged from the top at about 50 cm higher than the PMT glass envelopes. We tuned each LD's beam intensity with a width of 150 ps so that the occupancy in a PMT was as low as about 0.09 photoelectron/hit to generate mostly SPE. The peak wavelength of the LD's was set to 405 nm. The room temperature was monitored to be stable around 25 °C.

2.1.1 Systematic Uncertainty Reduction

Although we have applied Helmholtz coils to neutralize the geo-magnetic field, still the magnetic field at each channel was not perfectly zero and variance remained. Fig.2 shows the variance in the magnetic field measured at the center of each channel. Such a non-uniformity might be caused by the ferromagnetic sources inside the laboratory that could not be easily removed. The photoelectrons propagated roughly along the Z direction and thus the field variance in this direction was not strictly constrained.

During the experiment, we placed the reference PMT at the other six channels and positions to know the difference in measurements. The data of the reference PMT taken at all seven channels were then used to reduce the systematic uncertainties, which includes the different magnetic fields, signal amplification, and electronic noises.

3. Data Analysis

3.1 SPE Fitting

An example from B&L PMT EA4790-E is shown in Fig.3. To fit the charge distribution of the SPE peak from ADC, we used Eq.(1)

$$f(x) = p_0 \cdot e^{-\left(\frac{x-p_1}{\sqrt{2}p_2}\right)^2} + 0.5 \cdot p_3 \cdot \left(\text{erf}\left(\frac{x-p_4}{p_5}\right) - \text{erf}\left(\frac{x-p_1}{p_2}\right) \right) \quad (1)$$

where the p_i 's are free parameters and the error function erf was included for the back scattering on the first dynode. The SPE charge resolution was defined as the ratio of Gaussian peak width to its peak position, i.e. p_2/p_1 .

For the time distribution, an Exponentially Modified Gaussian distribution was used.

$$f(x) = 0.5 \cdot \lambda \cdot \gamma \cdot e^{0.5 \cdot \lambda \cdot (2 \cdot \mu + \lambda \cdot \sigma^2 - 2x)} \cdot \left(1 - \text{erf} \left(\frac{\mu + \lambda \cdot \sigma^2 - x}{\sqrt{2} \sigma} \right) \right) \quad (2)$$

where μ , λ , σ , and γ are the free parameters of fitting. We used the FWHM of the time peak in Fig.3 to represent the Transit Time Spread (TTS) of photoelectrons inside a PMT, which is a direct measurement of PMT's time resolution.

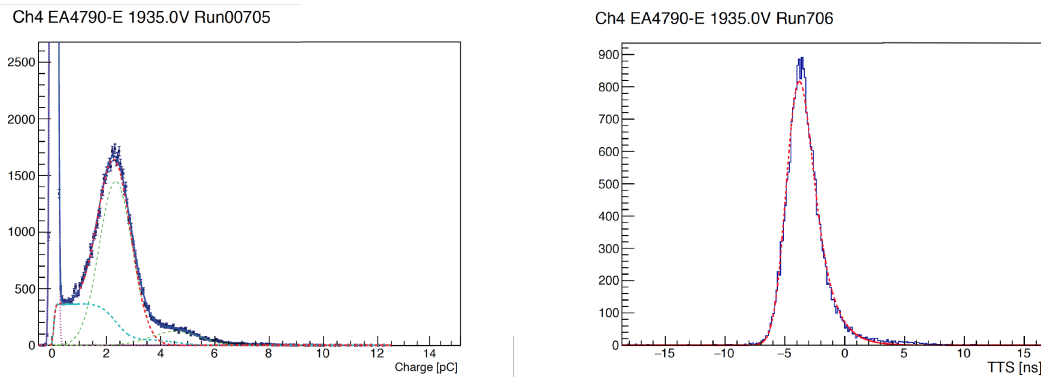


Fig. 3. Left Panel: SPE charge distribution; right panel: SPE time distribution. Red dashed curves represent the fitting results of Eq. (1) and Eq. (2) respectively.

3.2 Voltage Scan

To find the voltage needed for the PMT, we scanned each tube with twelve voltages ranging from 1500V to 2250V. From the fitted SPE peaks by Eq. (1), we determined the voltage dependence of gain with

$$\mu(V) = \alpha \cdot (V - V_{\text{off}})^{\beta} \quad (3)$$

where $\mu(V)$ is the gain corresponding to voltage V ; α , β , and V_{off} are the parameters calculated by the data fitting. The target voltage determined in this experiment corresponds to 1.4×10^7 gain.

3.3 Dark Rate

We set the discriminator threshold to 1 mV, which corresponds roughly to 0.25 PE, and counted the hit rate above the threshold in each PMT with no light. The dark rate mean at around 15 kHz was almost four times the current value of 4 kHz inside the SK tank. However, the measurement of dark rate this time do not fully represent the quality of the HK B&L PMTs since the room temperature was about 10 °C higher than water temperature and the PMTs were not completely stabilized.

3.4 Results

During the experiment there were six SK PMTs taken out temporarily from the SK tank and we measured them with the same set up. The results are shown in Table.1. The SPE signal of an HK B&L PMT is more recognizable than the SK one's with a superior performance in SPE charge and time resolution.

Fig.4 presents the measurements and the selection of all B&L PMTs based on the target voltage, SPE time resolution, SPE charge resolution, and dark rate. The allowed range for each quantity, represented by the dashed vertical lines in Fig.4, was (1500, 2450) V, (1, 4) ns, (20, 70)%, and (2, 30) kHz respectively.

	SK PMT	HK PMT
Time Resolution (ns)	6.73	2.59
Charge Resolution	60.1%	30.8%

Table I. The comparison is based on the averages of six SK Venetian blind PMTs and 145 HK B&L PMTs at 1.4×10^7 gain.

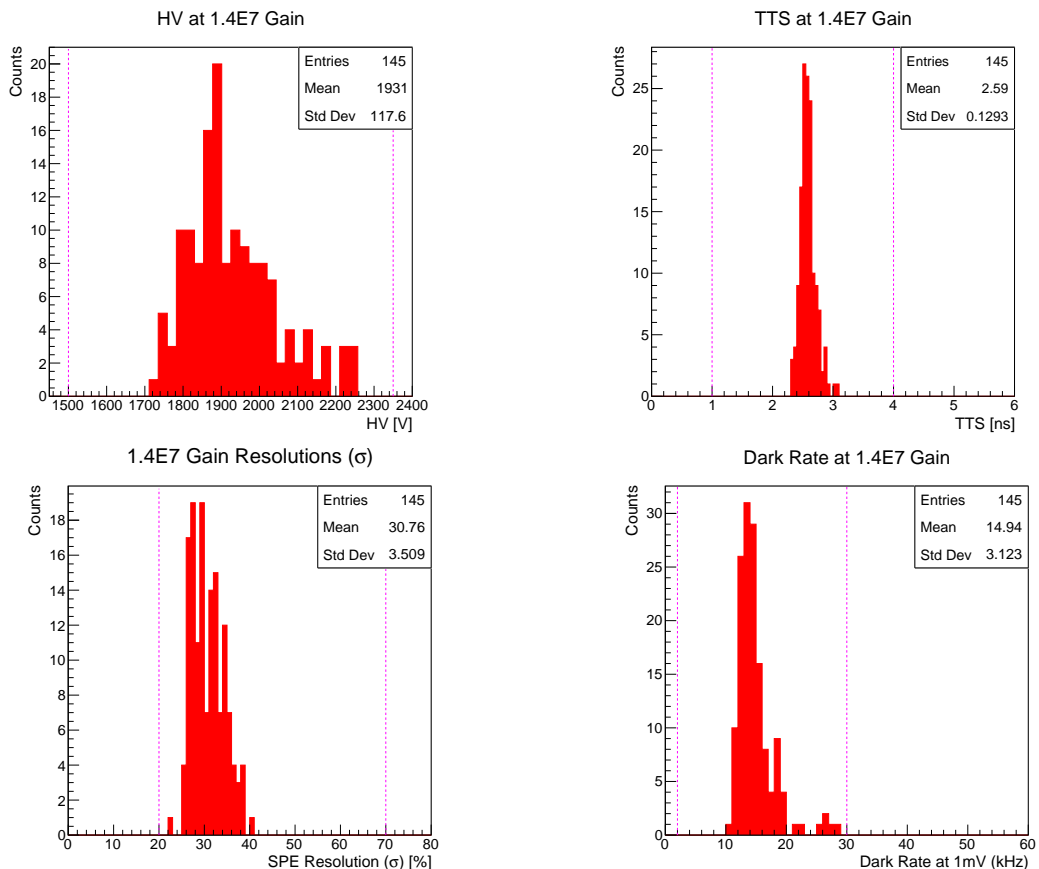


Fig. 4. The measurement results of all B&L PMTs with selection ranges shown in dashed lines. Based on the 4 measurements, all B&L PMTs were qualified to be installed in SK.

4. Conclusion

From our measurement, we have confirmed that all received 50 cm HK B&L PMTs have passed the check before installation with reasonable individual differences. Considering the lower temperature in the SK tank, we expect even a better performance of these 50 cm B&L PMTs in the future long-term operation.

References

[1] K. Abe *et al.* (Hyper-Kamiokande Proto-Collaboration), "Hyper-Kamiokande Design Report", arXiv:1805.04163v1, 2018.